Optomechanical Quantum Entanglement Mediated by Acoustic Phonon Fields

Qidong Xu[*] and M. P. Blencowe[†]

Department of Physics and Astronomy, Dartmouth College, Hanover, New Hampshire 03755, USA

We present exact solutions for the quantum time evolution of two spatially separated, local inductor-capacitor (LC) oscillators that are coupled optomechanically to a long elastic strip that functions as a quantum thermal acoustic field environment. We show that the optomechanical coupling to the acoustic environment gives rise to causal entanglement dynamics between the two LC oscillators in the absence of resonant photon exchange between them, and that significant entanglement develops regardless of the environment temperature. Such a process establishes that distributed entanglement may be generated between superconducting qubits via a connected phonon bus bar, without the need for resonant phonon release and capture.

Introduction.—Thermal environments have often been invoked to explain the decoherence of a quantum system, thus, resulting in the observed classical, macroscopic world [1–3]. However, it is also well known that thermal environments can generate quantum entanglement when coupled to otherwise independent quantum subsystems under suitable conditions [4–15]; several experimental realizations have been proposed [4,16–19], with further examples considered in the Ref. [20] review (and references therein).

In this Letter, we investigate the entanglement dynamics of an experimentally feasible model comprising two spatially separated local inductor-capacitor (LC) oscillators that are capacitively coupled to a long, partially metallized elastic strip via the optomechanical interaction [21]; here, the elastic strip functions as a thermal acoustic phonon environment. Hybrid quantum information platforms with acoustic phonons serving as the mediators have received increasing attention in recent years [22–25], in part, due to their long coherence times [26] and much lower propagation speeds compared with photons [27]. While most studies have focused on single mode resonant phonon dynamics models, instead, we adopt a field theoretic description of the elastic strip in our model, which naturally leads to local, spatially dependent nonresonant couplings between the oscillators and the phonon field. This then allows for an explicit analysis of the causal nature of the entanglement dynamics between the two oscillators arising from the finite acoustic wave propagation speed in the elastic strip. Tracing out the elastic strip (phonon) degrees of freedom, we solve exactly for the quantum time evolution of the LC oscillators, with particular attention paid to the competing entanglement and dephasing or rephasing dynamics of the LC oscillators. In particular, we find that the two LC oscillators can become substantially entangled due to their couplings to the much

lower frequency acoustic phonon modes, which can be engineered to have significantly low transmission loss rates [28].

With the capacitor sizes much smaller than the elastic strip length, the two LC oscillators can also be thought of as variants of the so-called Unruh-DeWitt (UDW) photon detector model [29–31]; we find that the entanglement only forms between the two LC oscillators when they are "timelike" separated (i.e., causally connected), as opposed to "spacelike" separated, with respect to the acoustic wave propagation (i.e., phonon) speed. This is to be contrasted with the results obtained for the usually considered bilinear type interaction between the UDW detectors and the field, where entanglement can be "harvested" from the field vacuum state even for spacelike separated detectors [32–36]. Such a difference lies in the fact that the optomechanical interaction commutes with the free Hamiltonian of the LC oscillators and, therefore, obeys the general no-go theorem of Ref. [37] for entanglement generation when the two detectors are spacelike separated.

The optomechanical interaction bears some similarities with the weak field, scalar matter-graviton interaction action [38,39]. In particular, our model Hamiltonian [see Eq. (3)] takes on the same form as considered in recent proposals [40,41] to observe quantum gravity induced entanglement at low energies [42]. Therefore, the model can serve as a gravitational entanglement generation analog to explicitly inform how the mediating field is responsible for the entanglement generation, in contrast to these proposals where only the effective Newtonian potential was considered.

The model.—Our model scheme (Fig. 1) builds on the one considered in Ref. [43], which investigated dephasing only of a single LC oscillator coupled capacitively to a long elastic strip. In particular, we consider two identical LC circuits separated by a distance D, each coupled
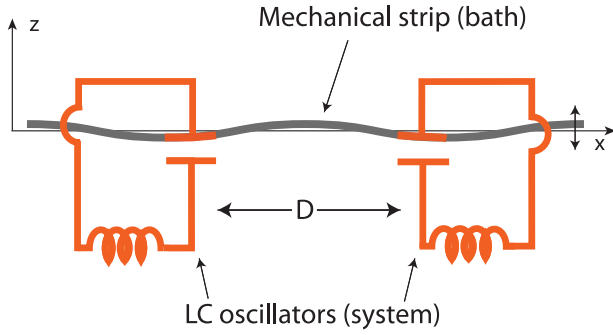
FIG. 1. Scheme of the model system. Two spatially separated *LC* circuit oscillators (system) are capacitively coupled to a long oscillating, elastic strip (environment) via two metallized segments.

capacitively via metallized segments (with lengths ΔL) of a long, elastic mechanical strip with overall length $L > D \gg \Delta L$ that is clamped at both ends. The *LC* circuits are sited such that the center point between the two capacitors coincides with the strip center. The transverse width (W) and thickness (T) of the strip satisfy $T \ll W \ll L$. The indicated lower capacitor plates are assumed fixed, also with length ΔL, the same width W as the strip, and separated from the upper flexing, metallized ΔL strip segments of the strip by a small equilibrium vacuum gap $d \ll W$. The bare, zero flexing capacitance of each *LC* circuit is then given by the standard parallel plate expression $\mathsf{C}_b = \epsilon_0 W \Delta L / d$ with ϵ_0 the vacuum permittivity. In the following, we shall denote the left circuit capacitance by C_l and right circuit capacitance by C_r, and we denote both circuit inductances by L.

Neglecting displacements in the transverse y and longitudinal x directions, the flexing mechanical displacement of the strip along the transverse z direction can be described by the Hamiltonian

$$\mathcal{H}_{\text{bath}} = \frac{\rho_m WT}{2} \int_0^L dx \left(\frac{\partial u_z}{\partial t} \right)^2 + \frac{F}{2} \int_0^L dx \left(\frac{\partial u_z}{\partial x} \right)^2, \quad (1)$$

where $u_z(t,x)$ is the displacement field, ρ_m is the mass density of the strip, and we assume a sufficiently large tensile force F is applied at both ends of the strip so that it behaves effectively as a string with end boundary conditions $u_z(t, x = 0) = u_z(t, x = L) = 0$.

The Hamiltonian for the two *LC* circuit system is

$$\mathcal{H}_{\text{sys}} = \frac{Q_l^2}{2\mathsf{C}_l} + \frac{\Phi_l^2}{2\mathsf{L}} + \frac{Q_r^2}{2\mathsf{C}_r} + \frac{\Phi_r^2}{2\mathsf{L}}, \quad (2)$$

where Q is the capacitor charge coordinate and Φ is the inductor flux coordinate with subscript l and r denoting left and right circuit, respectively. We note that C_l and C_r are implicit functions of the displacement field $u_z(t,x)$, with $\mathsf{C}_l(u_z = 0) = \mathsf{C}_r(u_z = 0) \equiv C_b$.

Introducing creation or annihilation operators for both the *LC* circuits and the elastic strip modes, and expanding the *LC* circuit resonant frequencies and creation or annihilation operators to first order in the strip transverse displacement field with the usual rotating wave approximations, the total Hamiltonian reduces to the standard optomechanical Hamiltonian [43]

$$\mathcal{H} = \sum_{k=1}^{2} \left[\hbar \Omega_b \left(a_k^\dagger a_k + \frac{1}{2} \right) + \sum_{j=1}^{\infty} \hbar g_{k,j} \left(a_k^\dagger a_k + \frac{1}{2} \right) (b_j + b_j^\dagger) \right] + \sum_{j=1}^{\infty} \hbar \omega_j \left(b_j^\dagger b_j + \frac{1}{2} \right), \quad (3)$$

where a_k ($a_k^\dagger$) are the annihilation (creation) operators for the *LC* oscillators with bare frequency $\Omega_b = 1/\sqrt{\mathsf{C}_b \mathsf{L}}$, with the subscript $k = 1(2)$ denoting, respectively, the left (right) *LC* oscillator, and b_j ($b_j^\dagger$) are the annihilation (creation) operators for the elastic strip modes of frequency $\omega_j = \pi j \sqrt{(F/2mL)}$, with $m = \rho_m WTL/2$ the effective mass of the modes. The coupling strength between each *LC* oscillator and the elastic strip modes is approximately given by [43]

$$g_{1(2),j} = -\frac{\Omega_b}{2d} \left(\frac{\hbar}{2m\omega_j} \right)^{1/2} \sin \left(\frac{\pi j}{L} \times \frac{L \mp D}{2} \right), \quad (4)$$

where we have taken the pointlike limit for the capacitors ($\Delta L \to 0$) utilizing the fact that ΔL is assumed to be much smaller than the length L of the strip; there is no ultraviolet (UV) divergence in such a limit in the determination of the quantum dynamics of the *LC* oscillator systems given below, which is a consequence of the effective one dimensional nature of the elastic strip [43]. The coupling strength (4) allows closed form analytical solutions for the quantum dynamics.

Supposing that the *LC* oscillators and the elastic strip are prepared initially at $t = 0$ in a product state with the latter in a thermal state, the time evolution of the reduced oscillator system density matrix expanded in the Fock state basis can be expressed as follows (for derivation details, see Supplemental Material [44]):

$$\rho_{n_1 n_2, n'_1 n'_2}(t) = \exp\{-it\Omega_b(n_1 + n_2 - n'_1 - n'_2) + ip_1(t)[(n_1 + n'_1 + 1)(n_1 - n'_1) + (n_2 + n'_2 + 1)(n_2 - n'_2)]$$
$$+ ip_2(t)[2n_1 n_2 - 2n'_1 n'_2 + n_1 + n_2 - n'_1 - n'_2] - d_1(t)[(n_1 - n'_1)^2 + (n_2 - n'_2)^2]$$
$$- d_2(t)(n_1 - n'_1)(n_2 - n'_2)\}\rho_{n_1 n_2, n'_1 n'_2}(0), \tag{5}$$

where the respective time-dependent terms are given by

$$p_1(t) = \lambda\left\{\frac{\pi^2\tau}{6} - \tau\mathrm{Re}[\mathrm{Li}_2(-e^{i\sigma})] + \mathrm{Im}\left[\frac{1}{2}\mathrm{Li}_3(-e^{i(\tau+\sigma)})\right.\right.$$
$$\left.\left. + \frac{1}{2}\mathrm{Li}_3(-e^{i(\tau-\sigma)}) - \mathrm{Li}_3(e^{i\tau})\right]\right\}, \tag{6a}$$

$$p_2(t) = \lambda\left\{\frac{\pi^2\tau}{12} + \tau\mathrm{Re}[\mathrm{Li}_2(e^{i\sigma})] - \mathrm{Im}\left[\mathrm{Li}_3(-e^{-i\tau})\right.\right.$$
$$\left.\left. + \frac{1}{2}\mathrm{Li}_3(e^{i(\tau-\sigma)}) + \frac{1}{2}\mathrm{Li}_3(e^{i(\tau+\sigma)})\right]\right\}, \tag{6b}$$

$$d_1(t) = \sum_{j=1}^{\infty}\frac{1 - \cos(\omega_j t)}{\omega_j^2}g_{1,j}^2\coth\left(\frac{\beta\hbar}{2}\omega_j\right), \tag{6c}$$

$$d_2(t) = 2\sum_{j=1}^{\infty}\frac{1 - \cos(\omega_j t)}{\omega_j^2}g_{1,j}g_{2,j}\coth\left(\frac{\beta\hbar}{2}\omega_j\right), \tag{6d}$$

with $\beta^{-1} = k_B T$, where k_B is Boltzmann's constant and T is the elastic strip (environment) temperature. The dimensionless numerical constant $\lambda = \Omega_b^2\hbar/(16d^2 m\omega_1^3)$, and $\mathrm{Li}_s(\cdot)$ is the polylogarithm function of order s. Note that, in the above expressions, we have also introduced the following notations for the dimensionless time: $\tau = \omega_1 t$, and for the scaled distance ratio: $\sigma = \pi D/L$.

Now, we make several observations based on the form of Eq. (5) about the reduced system dynamics of the LC oscillators. Apart from the free evolution term, the $p_1(t)$ and $d_1(t)$ terms correspond to environment induced renormalization and dephasing, respectively, of the individual LC oscillators, while the $p_2(t)$ and $d_2(t)$ terms encode the effective environment induced mutual dynamics between the two LC oscillators. In particular, we have competing processes, here, where a nonzero mutual phase term $p_2(t)$ can render the reduced density matrix of the LC oscillators to be entangled, while the real dephasing terms $d_1(t)$ and $d_2(t)$ serve to counteract the entanglement generation. However, since both the $d_1(t)$ and $d_2(t)$ terms contain the oscillating factor $1 - \cos(\omega_j t)$, in which the harmonic mechanical mode frequencies are equally spaced, these two terms completely vanish at times $t = 2\pi j/\omega_1$, $j = 0, 1, 2, \ldots$. This periodic, full rephasing phenomenon is crucial for the formation of entanglement as we will see below; in particular, it allows for periodic time windows in which to probe the generated entanglement. We note that this full rephasing phenomenon is a consequence of the one

dimensional nature of the long elastic strip with uniformly spaced vibrational modes; only partial rephasing will occur for two dimensional, elastic membranes that have nonuniformly spaced vibrational modes [43].

A closer look at the $p_2(t)$ term also reveals that it enforces causality for the model; this can be seen by performing a partial trace over one of the LC oscillator subsystems and noticing that its influence on the other oscillator is only through the $p_2(t)$ term. Causality requires that the physical state of one LC circuit will not be changed by the presence of the other within the time that it takes for phonons to travel the separation distance between the two capacitors: $\Delta t = (D/v_{\mathrm{ph}}) = \sqrt{(2m/FL)}D$, where $v_{\mathrm{ph}} = \sqrt{(FL/2m)}$ is the phonon speed. Considering the following inequalities for τ and σ: $\tau < \sigma$ (corresponding to $t < \Delta t$) and $\sigma < \pi$ (corresponding to $D < L$), $p_2(t)$, in Eq. (6b), can be rewritten as a combination of Bernoulli polynomials that are verified to vanish exactly and become nonzero only when $t > \Delta t$. We stress that such a causally consistent result can only be obtained by an exact, field theoretic treatment of the environment [47,48] (see Supplemental Material for further details [44]).

Zero temperature entanglement dynamics.—Now, we discuss the entanglement dynamics of the model. Since the interaction Hamiltonian commutes with the system Hamiltonian, entanglement can be realized only if both LC circuits are initially in a Fock state superposition. For simplicity, we shall consider an initial ($t = 0$) superposition of zero and single photon states for each LC circuit: $|\psi(0)\rangle = \frac{1}{2}(|0\rangle_l + |1\rangle_l) \otimes (|0\rangle_r + |1\rangle_r)$. Furthermore, we assume, as before, for calculational convenience, that the LC oscillators and strip are initially in a product state. The latter is equivalent to suddenly switching on the optomechanical interaction at $t = 0$. While unphysical (the capacitive couplings are always "on"), such an assumption may be justified by supposing that the LC oscillator superposition states are prepared on a timescale that is much shorter than the phonon travel time between the two oscillators.

First, we shall focus on the zero temperature limit for the phonon field (corresponding to the vacuum field state of the elastic strip). Despite the zero temperature limit being a challenge to realize given the presence of low frequency modes of the long strip, it allows analytical expressions for the dephasing terms (see Supplemental Material [44]), and yields important information about the competition between dephasing and entanglement generation.
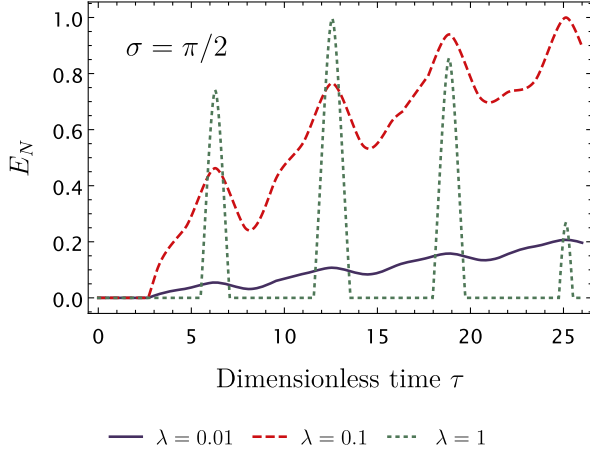
FIG. 2. Logarithmic negativity plotted as a function of dimensionless time $\tau = \omega_1 t$ with different values of the numerical constant λ. The parameter $\sigma = \pi/2$ (corresponding to the separation $D = L/2$) of the LC circuits.

To determine whether the system is entangled, we utilize the logarithmic negativity $E_N(\rho)$ [49] as our entanglement measure.

With the full time evolution of the system density matrix given by Eq. (5) and the calculated time dependent terms, we obtain the logarithmic negativity E_N as a function of the dimensionless time $\tau = \omega_1 t$ shown in Fig. 2; it can be seen that the entanglement dynamics is sensitive to the value of the numerical constant λ, with several features in the time dependence noted as follows: (1) For the parameters considered here, the entanglement can only build up some time later than $t = \Delta t$ (corresponding to $\tau = \sigma$) in the timelike regime with respect to the phonon speed v_{ph}; this is a combined consequence of causality and the effect of zero temperature dephasing; although the environment induced phase term $p_2(t)$ starts to build up immediately after $t = \Delta t$, some additional time may be required in order to overcome the dephasing for entanglement to develop between the two subsystems. (2) E_N is a local maximum at $\tau = 2j\pi$, $j = 1, 2, 3, \ldots$, corresponding to when both $d_1(t)$ and $d_2(t)$ vanish exactly, as noted previously. Furthermore, depending on the value of the numerical constant λ, E_N can get close to its upper bound value $= 1$ for the two-level bipartite system, signaling a maximally entangled system state. (3) With the periodic vanishing of the dephasing terms, the maximally entangled state can always be generated regardless of the separation distance between the LC circuits; a larger separation distance only results in a longer time for the entanglement to build up.

Entanglement dynamics with realistic conditions.—Now, we turn our attention to more realistic scenarios where the strip has a finite temperature and both LC oscillators are subject to external dissipation, characterized by an assumed common decay rate κ. Considering the frequency of the LC oscillators to be in the ~10 GHz regime with $\Omega_b \gg \kappa$, and

the device temperature to be in the ~10 mK regime, the dissipative quantum dynamics can be approximately described by the following zero temperature quantum master equation [50]:

$$\dot{\rho}_T = -i[\mathcal{H}, \rho_T] + \sum_{k=1}^{2} \kappa \mathcal{D}[a_k]\rho_T, \qquad (7)$$

where $\mathcal{H}$ is given by Eq. (3), ρ_T is the total density operator of the LC oscillators and the phonon field, and the superoperator is given by $\mathcal{D}[O]\rho_T = O\rho_T O^\dagger - \{O^\dagger O, \rho_T\}/2$. Assuming the same initial superposition state as previously for the LC oscillators and in the short time limit $\kappa t \ll 1$, the reduced density matrix of the two LC oscillators can be approximately obtained as the undamped solution of Eq. (5) plus an external environment induced perturbation term ρ_κ, which is given by (for derivation details, see Supplemental Material [44])

$$\rho_{\kappa n_1 n_2, n_1' n_2'} = \kappa h(t)\left[\sqrt{(n_1 + 1)(n_1' + 1)}\rho(t)_{n_1+1 n_2, n_1'+1 n_2'}\right.$$
$$\left. + \sqrt{(n_2 + 1)(n_2' + 1)}\rho(t)_{n_1 n_2+1, n_1' n_2'+1}\right]$$
$$- \frac{\kappa t}{2}(n_1 + n_1' + n_2 + n_2')\rho(t)_{n_1 n_2, n_1' n_2'}, \qquad (8)$$

where $h(t) = \int_0^t dt' e^{-2i(n_1 - n_1')p_1(t') - 2i(n_2 - n_2')p_2(t')}$, with $p_1(t)$ and $p_2(t)$ given by Eq. (6a) and Eq. (6b).

In the case of a finite temperature strip, the entanglement can be strongly suppressed due to the much more rapid thermal dephasing as compared with the zero temperature limit. However, the entanglement can, nonetheless, be present in the system around the times $\tau = 2j\pi$, $j = 1, 2, 3\ldots$ when there is full rephasing. On the other hand, the dissipation of the LC oscillators due to their external environments will eventually destroy any possible entanglement in the system; therefore, we shall only focus on the first peak of the entanglement when $\tau = 2\pi$. In order to quantitatively investigate the entanglement dynamics, we assume some example parameters for the model that are related to actual experimental devices. In particular, for the elastic strip we adopt the silicon nitride vibrating string parameters from Ref. [51]: $\rho_m = 10^3$ kg/m³, $F = 10^{-5}$ N, $W = 1$ μm, $T = 0.1$ μm; however, we assume a much longer length $L = 2$ cm than that considered in Ref. [51] ($\approx$60 μm) corresponding to the lowest mechanical mode frequency $\omega_1 \approx 50$ kHz. For the LC oscillators, we adopt typical superconducting microwave LC circuit parameters with $\Delta L = 1$ μm, $d = 0.1$ μm, and the circuit mode frequency of $\Omega/(2\pi) = 15$ GHz. The separation distance between the capacitors is taken to be $D = 1$ cm. We shall consider a decay rate constant $\kappa \approx 1$ kHz; relaxation and dephasing times ranging from a few hundred microseconds to over a millisecond have been reported for superconducting circuits [52–56].
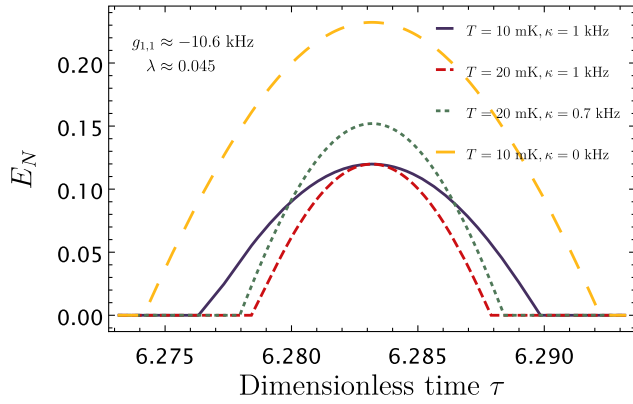
FIG. 3. Logarithmic negativity plotted as a function of dimensionless time $\tau = \omega_1 t$ for a range of acoustic phonon field temperatures and decay rates of the LC oscillators; the utilized parameters of the model discussed in the text correspond to $\lambda \approx 0.045$ and $g_{1,1} \approx -10.6$ kHz.

Using the above given parameters, we obtain the numerical results shown in Fig. 3 for the logarithmic negativity plotted around $\tau = 2\pi$, with a range of decay rates and temperatures achievable in a dilution refrigerator. Note that the amount of entanglement at $\tau = 2\pi$, when there is full rephasing [corresponding to $t \sim 126$ μs, which is within the short time range for obtaining the approximate solution of Eq. (8)], is not changed by the strip temperature (with the same decay constant). Instead, increasing the temperature narrows the time window (corresponding to a width around 250 ns for $T = 20$ mK in Fig. 3) during which the LC circuit system is entangled. On the other hand, increasing the decay rate causes both the entanglement maximum and time window width to decrease.

In order to experimentally probe the entanglement within the system, the state of the initial and final LC systems may, for example, be prepared and measured by coupling the LC circuits to driven nonlinear Josephson phase qubits [57,58]. We also note that, in the above analysis, we have ignored the loss channel due to the coupling of the acoustic strip modes to their external environments. This can be justified by noting that the quality (Q) factors of the low frequency mechanical modes may be engineered to have values as high as $Q = 8 \times 10^8$ [28], while the zero and single photon states of the LC oscillators induce strongly overlapping coherent states of the strip mechanical modes; such a decoherence channel can be safely ignored on the relevant timescales for entanglement formation (< 1 ms).

Conclusion.—We have investigated the entanglement dynamics of two LC oscillators coupled to a long elastic strip—a model system realization for two separated, localized UDW detectors interacting with a $1 + 1$ dimensional, massless scalar field. Exact solutions for the quantum time evolution of the oscillators were obtained, and the causality of the quantum dynamics analyzed.

With potential applications to quantum information processing in mind, it would be interesting to extend our model to multiple LC circuits and investigate possible multipartite entanglement generation via the optomechanical interaction [59] with a common, thermal acoustic environment, such as a long elastic strip or large surface area elastic membrane [43]. It would also be interesting to come up with ways to increase the coupling between the strip and the capacitors, thereby leading to stronger signatures of entanglement; larger effective optomechanical couplings can be achieved, for example, through the placement of a Cooper-pair transistor between the LC oscillator and gated mechanical strip [60], or by engineering a strong LC oscillator-transmission line photon "pressure" coupling for an all-microwave circuit realization [61,62].

[*] qidong.xu.gr@dartmouth.edu
[†] miles.p.blencowe@dartmouth.edu

[1] W. H. Zurek, Phys. Rev. D **26**, 1862 (1982).
[2] E. Joos and H. D. Zeh, Z. Phys. B Condens. Matter **59**, 223 (1985).
[3] W. H. Zurek, Phys. Today **44**, No. 10, 36 (1991).
[4] D. Braun, Phys. Rev. Lett. **89**, 277901 (2002).
[5] F. Benatti, R. Floreanini, and M. Piani, Phys. Rev. Lett. **91**, 070402 (2003).
[6] S. Oh and J. Kim, Phys. Rev. A **73**, 062306 (2006).
[7] R. Romano and D. D'Alessandro, Phys. Rev. Lett. **97**, 080402 (2006).
[8] A. Ferreira, A. Guerreiro, and V. Vedral, Phys. Rev. Lett. **96**, 060407 (2006).
[9] L. D. Contreras-Pulido and R. Aguado, Phys. Rev. B **77**, 155420 (2008).
[10] J. P. Paz and A. J. Roncaglia, Phys. Rev. Lett. **100**, 220401 (2008).
[11] D. P. S. McCutcheon, A. Nazir, S. Bose, and A. J. Fisher, Phys. Rev. A **80**, 022337 (2009).
[12] T. Zell, F. Queisser, and R. Klesse, Phys. Rev. Lett. **102**, 160501 (2009).
[13] F. Galve, L. A. Pachón, and D. Zueco, Phys. Rev. Lett. **105**, 180501 (2010).
[14] P. R. Eastham, P. Kirton, H. M. Cammack, B. W. Lovett, and J. Keeling, Phys. Rev. A **94**, 012110 (2016).
[15] L.-Z. Hu, Z.-X. Man, and Y.-J. Xia, Quantum Inf. Process. **17**, 1 (2018).
[16] A. Retzker, J. I. Cirac, and B. Reznik, Phys. Rev. Lett. **94**, 050504 (2005).
[17] C. Sabín, J. J. García-Ripoll, E. Solano, and J. León, Phys. Rev. B **81**, 184501 (2010).
[18] C. Sabín, B. Peropadre, M. del Rey, and E. Martín-Martínez, Phys. Rev. Lett. **109**, 033602 (2012).

[19] M. Cattaneo, G. L. Giorgi, S. Maniscalco, G. S. Paraoanu, and R. Zambrini, Ann. Phys. (Berlin) **533**, 2100038 (2021).

[20] L. Aolita, F. De Melo, and L. Davidovich, Rep. Prog. Phys. **78**, 042001 (2015).

[21] M. Aspelmeyer, T. J. Kippenberg, and F. Marquardt, Rev. Mod. Phys. **86**, 1391 (2014).

[22] A. Bienfait, K. J. Satzinger, Y. P. Zhong, H.-S. Chang, M.-H. Chou, C. R. Conner, É. Dumur, J. Grebel, G. A. Peairs, R. G. Povey, and A. N. Cleland, Science **364**, 368 (2019).

[23] M. Mirhosseini, A. Sipahigil, M. Kalaee, and O. Painter, Nature (London) **588**, 599 (2020).

[24] É. Dumur, K. J. Satzinger, G. A. Peairs, M.-H. Chou, A. Bienfait, H.-S. Chang, C. R. Conner, J. Grebel, R. G. Povey, Y. P. Zhong, and A. N. Cleland, npj Quantum Inf. **7**, 173 (2021).

[25] A. Zivari, N. Fiaschi, R. Burgwal, E. Verhagen, R. Stockill, and S. Gröblacher, arXiv:2204.05066.

[26] G. S. MacCabe, H. Ren, J. Luo, J. D. Cohen, H. Zhou, A. Sipahigil, M. Mirhosseini, and O. Painter, Science **370**, 840 (2020).

[27] P. Delsing, A. N. Cleland, M. J. A. Schuetz, J. Knörzer, G. Giedke, J. I. Cirac, K. Srinivasan, M. Wu, K. C. Balram, C. Bäuerle *et al.*, J. Phys. D **52**, 353001 (2019).

[28] A. H. Ghadimi, S. A. Fedorov, N. J. Engelsen, M. J. Bereyhi, R. Schilling, D. J. Wilson, and T. J. Kippenberg, Science **360**, 764 (2018).

[29] W. G. Unruh, Phys. Rev. D **14**, 870 (1976).

[30] B. S. DeWitt, Quantum gravity: The new synthesis, in *General Relativity: An Einstein Centenary Survey* (Cambridge University Press, Cambridge, England, 1979), pp. 680–745.

[31] S.-Y. Lin and B.-L. Hu, Phys. Rev. D **76**, 064008 (2007).

[32] B. Reznik, Found. Phys. **33**, 167 (2003).

[33] B. Reznik, A. Retzker, and J. Silman, Phys. Rev. A **71**, 042104 (2005).

[34] S.-Y. Lin and B. L. Hu, Phys. Rev. D **81**, 045019 (2010).

[35] E. Martín-Martínez, E. G. Brown, W. Donnelly, and A. Kempf, Phys. Rev. A **88**, 052310 (2013).

[36] G. Salton, R. B. Mann, and N. C. Menicucci, New J. Phys. **17**, 035001 (2015).

[37] P. Simidzija, R. H. Jonsson, and E. Martín-Martínez, Phys. Rev. D **97**, 125002 (2018).

[38] M. P. Blencowe, Phys. Rev. Lett. **111**, 021302 (2013).

[39] Q. Xu and M. P. Blencowe, arXiv:2005.02554.

[40] S. Bose, A. Mazumdar, G. W. Morley, H. Ulbricht, M. Toroš, M. Paternostro, A. A. Geraci, P. F. Barker, M. S. Kim, and G. Milburn, Phys. Rev. Lett. **119**, 240401 (2017).

[41] C. Marletto and V. Vedral, Phys. Rev. Lett. **119**, 240402 (2017).

[42] This can be most easily seen from a comparison of our Hamiltonian in Eq. (3) and Eq. (1) in the Supplemental Material for Ref. [40] where gravity, as the mediator of the entanglement, is treated as a quantum field.

[43] Q. Xu and M. P. Blencowe, Phys. Rev. A **104**, 063509 (2021).

[44] See Supplemental Material at http://link.aps.org/supplemental/10.1103/PhysRevLett.129.203604 for calculation details and further discussion on causality, which includes Refs. [45,46]).

[45] S. Bose, K. Jacobs, and P. L. Knight, Phys. Rev. A **59**, 3204 (1999).

[46] S. Mancini, V. I. Man'ko, and P. Tombesi, Phys. Rev. A **55**, 3042 (1997).

[47] R. H. Jonsson, E. Martin-Martinez, and A. Kempf, Phys. Rev. A **89**, 022330 (2014).

[48] D. M. T. Benincasa, L. Borsten, M. Buck, and F. Dowker, Classical Quantum Gravity **31**, 075007 (2014).

[49] G. Vidal and R. F. Werner, Phys. Rev. A **65**, 032314 (2002).

[50] C. Gardiner and P. Zoller, *Quantum Noise: A Handbook of Markovian and Non-Markovian Quantum Stochastic Methods with Applications to Quantum Optics* (Springer Berlin, Heidelberg, 2004).

[51] R. Schilling, H. Schütz, A. H. Ghadimi, V. Sudhir, D. J. Wilson, and T. J. Kippenberg, Phys. Rev. Appl. **5**, 054019 (2016).

[52] M. Reagor *et al.*, Phys. Rev. B **94**, 014506 (2016).

[53] A. Nersisyan *et al.*, in *2019 IEEE International Electron Devices Meeting (IEDM)* (IEEE, San Francisco, CA, 2019), pp. 31.1.1–31.1.4.

[54] K. X. Wei, I. Lauer, S. Srinivasan, N. Sundaresan, D. T. McClure, D. Toyli, D. C. McKay, J. M. Gambetta, and S. Sheldon, Phys. Rev. A **101**, 032343 (2020).

[55] H. Zhang, S. Chakram, T. Roy, N. Earnest, Y. Lu, Z. Huang, D. K. Weiss, J. Koch, and D. I. Schuster, Phys. Rev. X **11**, 011010 (2021).

[56] A. Somoroff, Q. Ficheux, R. A. Mencia, H. Xiong, R. V. Kuzmin, and V. E. Manucharyan, arXiv:2103.08578.

[57] M. Hofheinz, H. Wang, M. Ansmann, R. C. Bialczak, E. Lucero, M. Neeley, A. D. O'Connell, D. Sank, J. Wenner, J. M. Martinis, and A. N. Cleland, Nature (London) **459**, 546 (2009).

[58] A. Blais, A. L. Grimsmo, S. M. Girvin, and A. Wallraff, Rev. Mod. Phys. **93**, 025005 (2021).

[59] D. E. Bruschi, J. Math. Phys. (N.Y.) **60**, 062105 (2019).

[60] A. J. Rimberg, M. P. Blencowe, A. D. Armour, and P. D. Nation, New J. Phys. **16**, 055008 (2014).

[61] J. R. Johansson, G. Johansson, and F. Nori, Phys. Rev. A **90**, 053833 (2014).

[62] D. Bothner, I. C. Rodrigues, and G. A. Steele, Nat. Phys. **17**, 85 (2021).